Supplementary Material
A Revised Underwater Image Formation Model

Derya Akkaynak Tali Treibitz
University of Haifa
derya.akkaynak@gmail.com, ttreibitz@univ.haifa.ac.il

1. Dependency of β_c^B on Camera Response

In Sec. 3.2 of the main text, we presented the physically valid space of β_c^B, and identified its dependencies. Compared to β_c^D in [1] of main text, we noted that β_c^B was also sensitive to $S_c(\lambda)$, but only weakly. To clarify, β_c^B does vary with S_c, but it varies more with ambient light E (implicit in B^∞) which becomes increasingly monotonic with depth, making spectral dependence less important. To demonstrate this, we compiled the response of 74 cameras (Fig. 1a, black curves show light at the surface and 10m depth), and calculated the β_c^B locus (Fig. 1b&c). This dataset shows that despite the large variation across sensors, search space is reduced to the same part of the β_c^B domain. The source of camera response curves are given in Table 1.

2. Error Analysis: Current Vs. Revised Model

In the main text (Sec. 6 and Fig. 7), we used seven scenarios to analyze the errors stemming from the use of the current versus the revised underwater image formation models. Fig. 6a showed the ground truth values of β_c^B and β_c^D for these scenarios for Jerlov Type II, which represented absorption dominated water types (Types I-IB were almost identical). Here, in Fig. 2, we present what the values of these coefficients would have been for scattering-dominated water types.

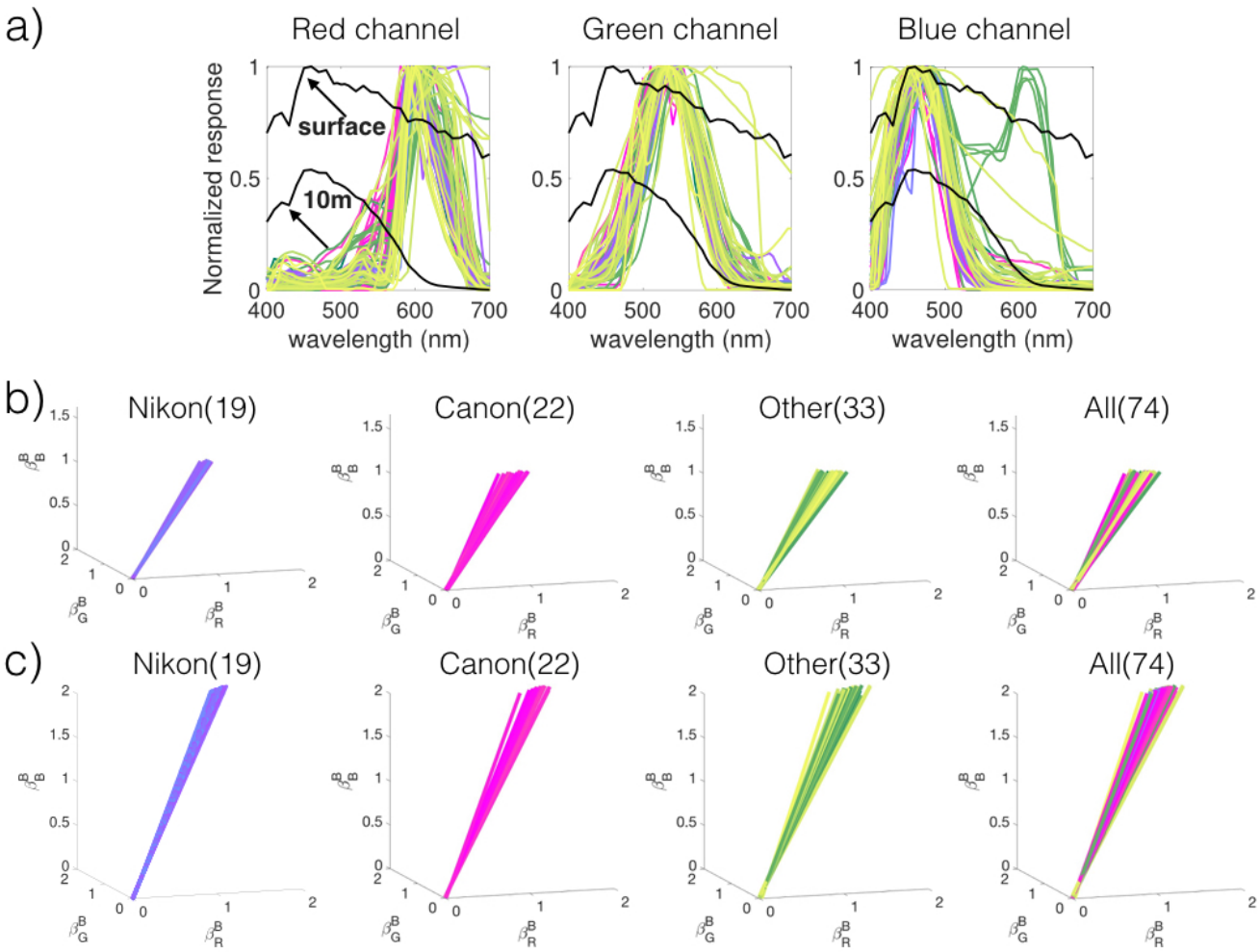

Figure 1. Extension of Fig. 4e in main text using the normalized response of 74 cameras **a)** Nikon (purple), Canon (pink), Other (green: Arriflex, Casio, Fuji, Hasselblad, Kodak, Leica, Manta, Nokia, Olympus, Panasonic, Pentax, Phase One, Point Gray, Sony, Sigma). Black curves show light at surface (D65) and attenuated at 10m for water type II (borderline between absorption and scattering dominated). The locus of β_c^B at 10m shows little variation for both **b)** absorption and **c)** scattering-dominated water types.

#	Make	Model	Source
1	Arriflex	D-21	[21]
2	Canon	1D Mk III	[16]
3	Canon	1Ds Mk II	[6]
4	Canon	5D	[14, 12]
5	Canon	5D Mk II	[16, 25]
6	Canon	10D	[17, 15]
7	Canon	20D	[16]
8	Canon	40D	[16, 21, 13]
9	Canon	50D	[16]
10	Canon	60D	[16]
11	Canon	300D	[16]
12	Canon	400D	[17, 23, 18]
13	Canon	500D	[16]
14	Canon	600D	[16]
15	Canon	A2200	[9]
16	Casio	EXF1	[14]
17	Fuji	S5Pro	[21]
18	Hasselblad	H2	[16]
19	Hasselblad	H3D	[21]
20	iPhone	5	[20]
21	Kodak	DCS200	[24]
22	Kodak	DCS420	[17, 24, 15]
23	Kodak	DCS460	[17]
24	Leica	M8	[21]
25	Manta	G032C	[3]
26	Nikon	D3	[16, 10]
27	Nikon	D3X	[16]
28	Nikon	D40	[16]
29	Nikon	D50	[16]
30	Nikon	D70	[17, 15]
31	Nikon	D80	[16]
32	Nikon	D90	[16]
33	Nikon	D100	[25]
34	Nikon	D200	[16, 21]
35	Nikon	D300s	[16]
36	Nikon	D700	[16, 21]
37	Nikon	D800	[22]
38	Nikon	D5000	[2]
39	Nikon	D5100	[16, 11]
40	Nikon	D7000	[23]
41	Nokia	1520	[8]
42	Nokia	N900	[16]
43	Olympus	EPL1s	[14]
44	Olympus	EPL2	[16]
45	Panasonic	DMCLX3	[21]
46	Panasonic	DMCLX5	[9]
47	Pentax	K5	[16]
48	Pentax	Q	[16]
49	Phase One	unspecified	[16]
50	Point Grey	Dragonfly express	[19]
51	Point Grey	Grasshopper 14S5C	[16]
52	Point Grey	Grasshopper 50S5C	[16]
53	Point Grey	Ladybug2	[17]
54	Red	Dragon	[4]
55	Sigma	Dp quattro	[5]
56	Sigma	SD Merill	[11]
57	Sony	DXC 930	[7]
58	Sony	Hypercam IMX178	[1]
59	Sony	NEX5N	[16]
60	Sony	NEX7	[9]

Table 1. Cameras in our compiled dataset of spectral responses.

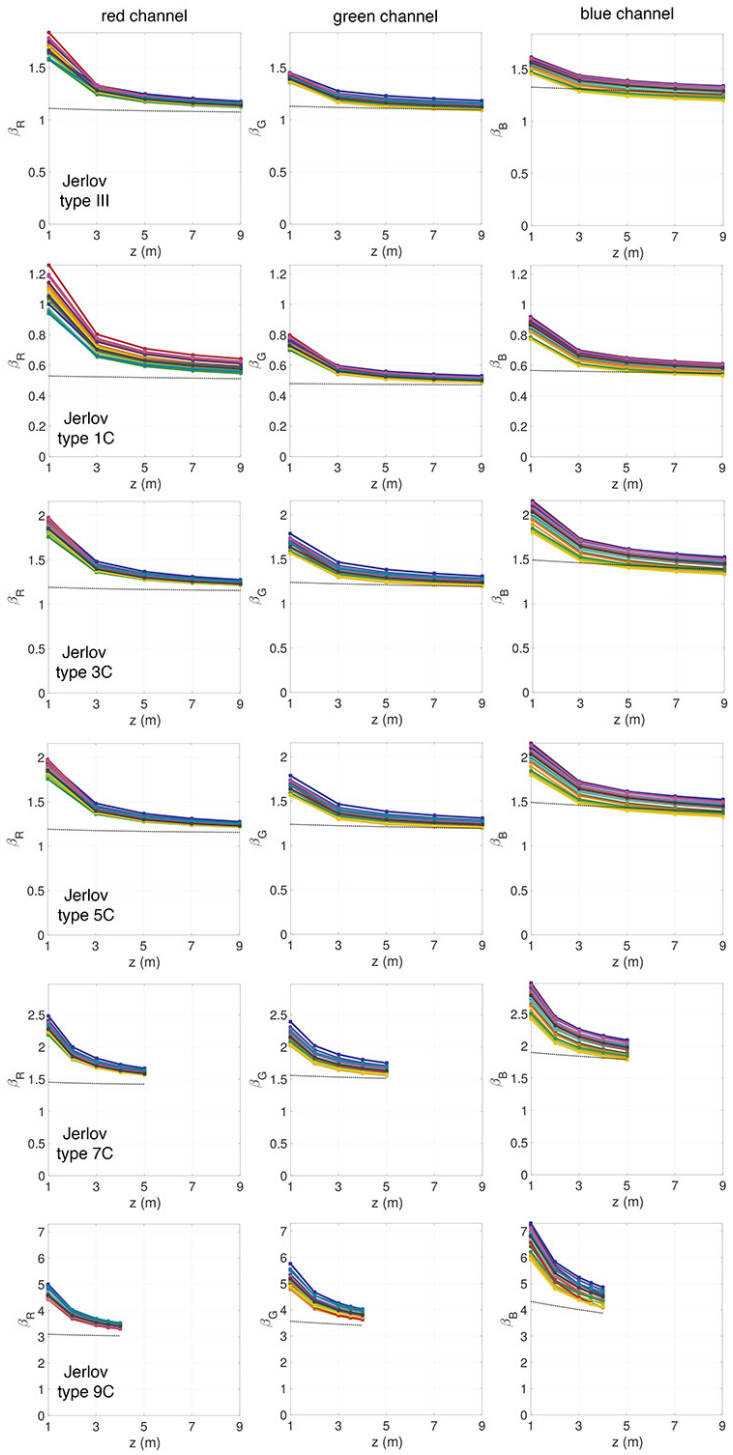

Figure 2. Values of β_c^D and β_c^B for scattering dominated water types (rows), shown for each color channel (columns). Note that for very turbid water types (7&9C) veiling light distance is already reached at 4-5m.

References

[1] http://altairastro.com. 3

[2] https://www.dxomark.com. 3

[3] http://www.alliedvision.com. 3

[4] http://www.red.com/. 3

[5] http://www.sigma-global.com. 3

[6] D. Akkaynak, E. Chan, J. J. Allen, and R. T. Hanlon. Using spectrometry and photography to study color underwater. In *Proc. MTS/IEEE OCEANS*, 2011. 3

[7] K. Barnard, F. Ciurea, and B. Funt. Sensor sharpening for computational color constancy. *JOSA A*, 18(11):2728–2743, 2001. 3

[8] P. Bartczak, A. Gebejes, P. Falt, J. Parkkinen, and P. Silfstein. Led-based spectrally tunable light source for camera characterization. In *Colour and Visual Computing Symposium (CVCS), 2015*, pages 1–5. IEEE, 2015. 3

[9] E. Berra, S. Gibson-Poole, A. MacArthur, R. Gaulton, and A. Hamilton. Estimation of the spectral sensitivity functions of un-modified and modified commercial off-the-shelf digital cameras to enable their use as a multispectral imaging system for uavs. *The International Archives of Photogrammetry, Remote Sensing and Spatial Information Sciences*, 40(1):207, 2015. 3

[10] M. Brady and G. E. Legge. Camera calibration for natural image studies and vision research. *JOSA A*, 26(1):30–42, 2009. 3

[11] M. M. Darrodi, G. Finlayson, T. Goodman, and M. Mackiewicz. Reference data set for camera spectral sensitivity estimation. *JOSA A*, 32(3):381–391, 2015. 3

[12] M. D. Fairchild. Seeing, adapting to, and reproducing the appearance of nature. *Applied optics*, 54(4):B107–B116, 2015. 3

[13] J. Garcia Mendoza. Characterisation of a multispectral digital camera system for quantitatively comparing complex animal patterns in natural environments. 2012. 3

[14] S. Han, Y. Matsushita, I. Sato, T. Okabe, and Y. Sato. Camera spectral sensitivity estimation from a single image under unknown illumination by using fluorescence. In *Proc. IEEE CVPR*, pages 805–812, 2012. 3

[15] C. P. Huynh and A. Robles-Kelly. Comparative colorimetric simulation and evaluation of digital cameras using spectroscopy data. In *Digital Image Computing Techniques and Applications, 9th Biennial Conference of the Australian Pattern Recognition Society on*, pages 309–316. IEEE, 2007. 3

[16] J. Jiang, D. Liu, J. Gu, and S. Susstrunk. What is the space of spectral sensitivity functions for digital color cameras? In *IEEE Workshop Applications of Computer Vision (WACV)*, pages 168–179, 2013. 3

[17] R. Kawakami, H. Zhao, R. T. Tan, and K. Ikeuchi. Camera spectral sensitivity and white balance estimation from sky images. *IJCV*, 105(3):187–204, 2013. 3

[18] V. Lebourgeois, A. Bégué, S. Labbé, B. Mallavan, L. Prévot, and B. Roux. Can commercial digital cameras be used as multispectral sensors? a crop monitoring test. *Sensors*, 8(11):7300–7322, 2008. 3

[19] M.-H. Lee, D.-K. Seo, B.-K. Seo, and J.-I. Park. Optimal illumination spectrum for endoscope. In *Frontiers of Computer Vision (FCV), 2011 17th Korea-Japan Joint Workshop on*, pages 1–6. IEEE, 2011. 3

[20] T. Leeuw. Crowdsourcing water quality data using the iphone camera. 2014. 3

[21] C. Mauer and D. Wueller. Measuring the spectral response with a set of interference filters. In *IS&T/SPIE Electronic Imaging*, pages 72500S–72500S. International Society for Optics and Photonics, 2009. 3

[22] V. Medina, T. Muller, D. Lafon-Pham, A. Paljic, and P. Porral. Objective colorimetric validation of perceptually realistic rendering: a study of paint coating materials. *Journal of Electronic Imaging*, 25(6):061609–061609, 2016. 3

[23] J. Troscianko and M. Stevens. Image calibration and analysis toolbox–a free software suite for objectively measuring reflectance, colour and pattern. *Methods in Ecology and Evolution*, 6(11):1320–1331, 2015. 3

[24] P. L. Vora, J. E. Farrell, J. D. Tietz, and D. H. Brainard. Image capture: simulation of sensor responses from hyperspectral images. *IEEE Transactions on Image Processing*, 10(2):307–316, 2001. 3

[25] D. Wu, J. Tian, B. Li, Y. Wang, and Y. Tang. Recovering sensor spectral sensitivity from raw data. *Journal of Electronic Imaging*, 22(2):023032–023032, 2013. 3